Movements induced on existing masonry buildings by the excavation of a station of Toulouse subway line B

F. Emeriault, T. Bonnet-Eymard & R. Kastner
URGC Géotechnique, INSA, Lyon, France

E. Vanoudheusden
Arcadis ESG, Toulouse, France

J.Y. de Lamballerie
Maîtrise d'œuvre du Métro de l'Agglomération Toulousaine, Toulouse, France

ABSTRACT: A case study of interaction between a deep excavation and existing buildings is presented in this paper. The Saint-Agne subway station of Toulouse (France) new line B has been realized with a diaphragm wall supported by up to three levels of steel struts. Two monitoring sections have been installed. Section 2 corresponds to "Greenfield" condition and includes one inclinometer, strut load measurements and precise levelling. Section 1 has approximately the same characteristics and measuring devices for the wall and struts but also includes precise levelling and horizontal extension and crack opening measurement devices installed on an existing one-storey brick building only 4.3 m away from the diaphragm wall. The comparison of the results of both sections shed some light on the impact of deep excavation on nearby structures.

1 INTRODUCTION

The estimation of the ground surface displacements (settlements and horizontal movements) induced by deep excavation has been the topic of continuous research effort. One can refer to the work of Peck (1969), Clough & O'Rourke (1990), Ou et al. (1993), Long (2001) or Moormann & Moormann (2002). The analysis is generally based on a large number of case studies corresponding to a wide panel of excavation and support techniques and ground conditions (from soft to stiff clays or sands). It appears that the maximum lateral wall movement δ_{hmax} is generally found, for stiff clays or sand, close to 0.2% of the excavation depth H. The maximum ground surface settlement δ_{vmax} is also found about 0.15% H. When the excavation is close to existing structures, the potential induced damage can be predicted from the semi-empirical approaches of Boscardin & Cording (1989) or Burland (1995) requiring the knowledge of the variation of δ_h and δ_v with the horizontal distance d from the wall.

Nevertheless, little attention has been paid to the soil-structure interaction phenomenon occurring between the retaining wall and the existing buildings. This communication presents the results of a case study on the new line B of Toulouse subway currently under construction and that should be achieved in 2007. In addition to the 12.6 km long tunnel, 21 stations have been realized, generally with diaphragm walls. The limitation of the impact of the excavation on existing buildings is a key issue because in most cases the stations are close to old buildings (especially in the city centre) made of brick.

The partners of the research project METROTOUL have been given the opportunity to install on the Saint-Agne station a completed set of measuring devices allowing to determine the effect of deep excavation of a nearby existing brick building. The results of this experimental campaign are presented in this paper.

2 SAINT-AGNE STATION

Saint-Agne station (part of Contract 5) is a 55.2 m × 17.15 m rectangular box with a 20.65 m long and 1 m thick diaphragm wall (Figure 1). The 17.2 m deep excavation requires the use of three levels of steel struts 0.61 or 0.66 m in diameter and 10.3 or 12.7 mm thick (Figure 2).

The encountered geology is homogeneous on the whole layout of the line B project. The tunnels run through the Toulouse molasses (hard sandy clay with pockets and lenses of very dense sand). Geotechnical investigations have shown that in these formations, K_0 is greater than 1, generally close to 1.2 and

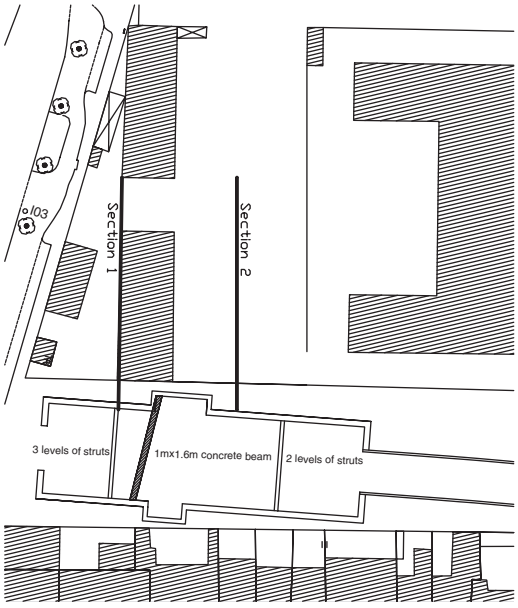

Figure 1. Global view of the site.

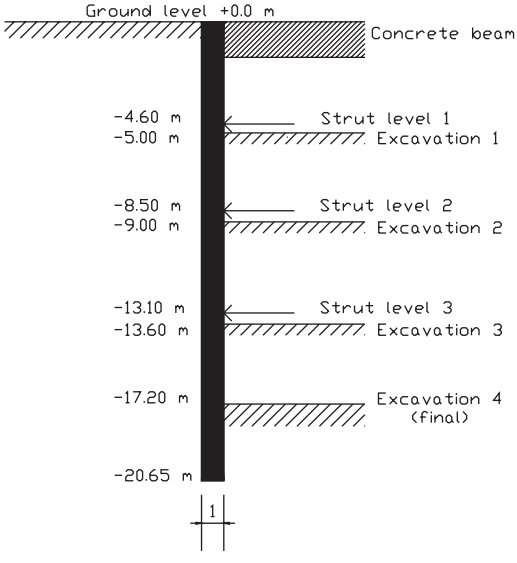

Figure 2. Cross-section of the diaphragm wall.

that geotechnical characteristics are homogeneous ($\gamma = 22\,\text{kN/m}^3$, $S_u = 300\,\text{kPa}$, $c' = 30\,\text{kPa}$, $\phi = 32°$). In the case of Saint-Agne station, the molasses are found between 1.2 and 2.0 m below ground level and the water table is approximately 2 m below ground level. Table 1 summarizes the different excavation phases and schedule.

Table 1. Excavation phases.

Phase n°	Date	Excavation level (m)	Strut level (m)
1-Excavation 1	18/06	−5.0	–
2-Strut 1	02/07	−5.0	−4.6
3-Excavation 2	11/07	−9.0	−4.6
4.1-Strut 2	08/09	−9.0	−8.5
4.2-Strut 2	09/09	−9.0	−8.5
5-Excavation 3	01/10	−13.6	−8.5
6-Strut 3	21/10	−13.6	−13.1
7-Excavation 4	28/11	−17.2	−13.1

Automatic strut load measurement starts on 24/07 and ends on 10/12.

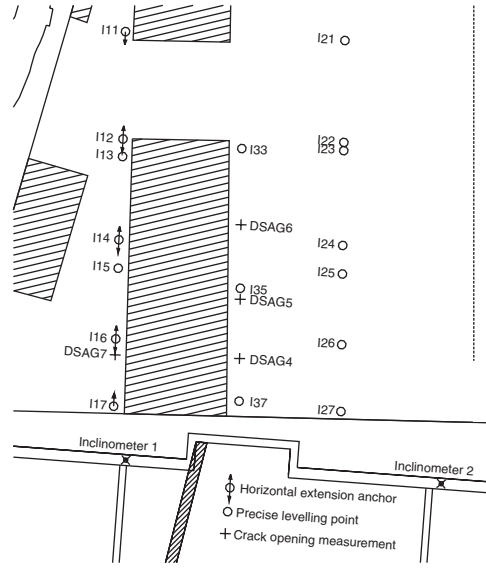

Figure 3. Location of the instrumentation.

3 DESCRIPTION OF THE MONITORING

Two fully equipped monitoring "sections" have been installed on the Saint-Agne excavation site (Figure 3): Section 2 corresponds to "Greenfield" conditions whereas Section 1 includes a 9 m × 27 m old brick building perpendicular to the excavation with a minimum distance to the diaphragm wall equal to 4.3 m.

Each section includes one inclinometer in the diaphragm wall, 4 vibrating wire strain gauges installed at mid-span on each of the three strut levels (with automatic data acquisition) and precise levelling. Horizontal extension of the brick building is measured on several intervals with an invar thread as well as crack opening with Demec strain gauges.

The data collected during all the construction phases (excavation, strut installation, slab concreting, strut

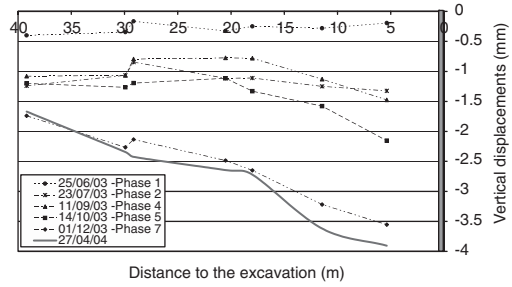

Figure 4. Greenfield settlement trough (points I21 to I27).

removal) are presented and analysed. The comparison of the results obtained for Sections 1 and 2 gives an insight on the soil-structure interaction phenomena induced by deep excavation close to existing buildings.

4 GREENFIELD SETTLEMENTS

For Section 2, precise levelling of 7 points (labelled I21 to I27 – see Figure 3) is performed at each step of the excavation. Figure 4 shows that the obtained settlement profiles are of the spandrel type. At the end of the excavation phases (28/11/03), a maximum settlement of 3.5 mm is obtained close to the top of the wall and at a distance of 40 m this settlement is only reduced to 1.5 mm.

In this case δ_{vmax}/H is approximately equal to 0.023%, which is very small compared to the average values of 0.15% reported by Clough & O'Rourke (1990) for stiff clays. This result can be partly explained by the high shear strength of the molasses and the rigidity of the 1m thick diaphragm wall.

A settlement influence zone can be estimated at 63 m, i.e. 3.7 H, which is greater than all the values reported by Peck (1969), Clough & O'Rourke (1990) or Hsieh & Ou (1998). The high K_0 value exhibited by the molasses (close to 1.2) can be responsible for this larger than usual extend of the excavation influence zone. Vanoudheusden et al. (2005) and Emeriault et al. (2005) have shown that this high K_0 is also responsible for horizontal movements larger than expected on several monitoring sections of tunnel and galleries of the subway line B.

Figure 4 also proves that the final settlement trough is quickly obtained at the end of the excavation phases: the trough measured after 5 months only departs from that observed at the end of Phase 7 by 0.35 mm.

5 BEHAVIOUR OF THE DIAPHRAGM WALL

The diaphragm wall itself is instrumented by two inclinometers while the different struts are equipped

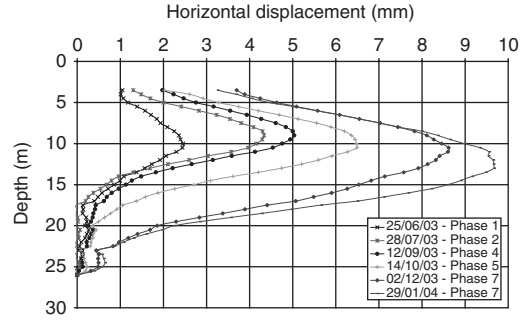

Figure 5. Horizontal displacements measured in Inclinometer 1.

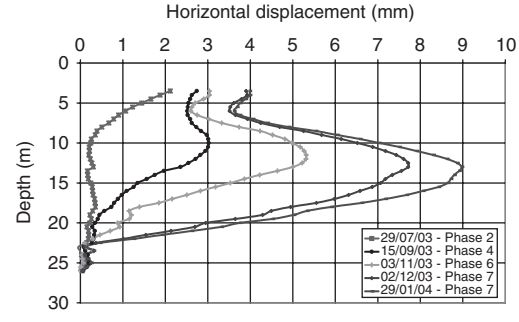

Figure 6. Horizontal displacements measured in Inclinometer 2.

with vibrating wire strain gauges (with automatic data acquisition)

Figures 5 and 6 present the horizontal displacement profiles obtained in inclinometers 1 and 2. A lack of grouting in the upper part of the inclinometer casings leads to discard all the values measured for the first 3 m.

Nevertheless, it appears that the movements obtained are very similar in shape and amplitude, the displacements being slightly greater in the case of Inclinometer 1 (δ_{hmax} is close to 8.6 mm instead of 7.7 mm for Inclinometer 2). The ratio δ_{hmax} / H equal to 0.05% should be compared with the average value of 0.2% reported by Clough & O'Rourke (1990).

Because the final embedded length of the wall is rather small (3.45 m), a global rotation movement is observed in the lower part of the wall and in the soil 2 m beneath the tip of the wall.

In the upper part of the diaphragm wall, a partial concrete slab (0.4 m thick) and a concrete beam (1.6 m high and 1 m thick) induce in the vicinity of Inclinometer 1 an increase in stiffness (cf. Figure 1). This explains that the behaviour of the top part of wall is mainly rotational whereas for the Inclinometer 2, the observed movement corresponds to a deflection towards the centre of the excavation.

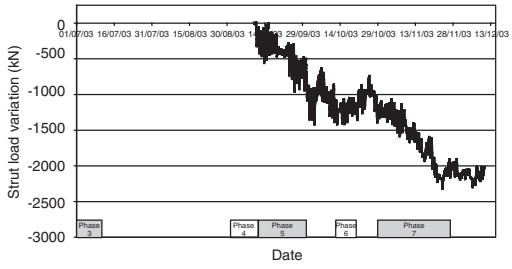

Figure 7. Normal force in strut 2-1.

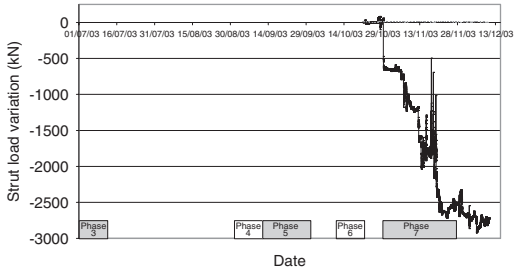

Figure 8. Normal force in strut 3-1.

Figures 5 and 6 also present the displacement profiles obtained after the construction of the slab and the removal of the lower level of struts. The maximum induced horizontal movements are close to 1 mm.

On each of the steel cylindrical struts, four vibrating wire strain gauges are installed at mid-span at 0°, 90°, 180° and 270°. Therefore, the axial force and bending moments in the vertical and horizontal plane can be calculated. In this paper, only the axial force will be considered.

For Section 1, the strut loads are monitored in the three levels of steel struts denoted 1-1 (upper), 2-1 (middle) and 3-1 (bottom). It is reminded that a 1 m × 1.6 m concrete beam is constructed across the excavation at the top of the diaphragm wall and that the load carried by this beam is not measured.

For Section 2, two levels of struts are used (denoted 2-2 and 3-2), a partial concrete slab is constructed at the top of the wall at the end of Phase 3. Figures 7 and 8 show that the different excavation phases lead to an increase in struts load (with a stable value obtained within a week after the excavation). They also show that the daily variations of axial load in the struts induced by the temperature and sunlighting range from 50 to 100 kN. The load carried by Strut 1-1 are not presented because they remain relatively small (less than 500 kN) throughout the different excavation phases.

Figure 9 summarizes the measured strut loads at the end of Phases 4, 6 and 7 and two weeks after the

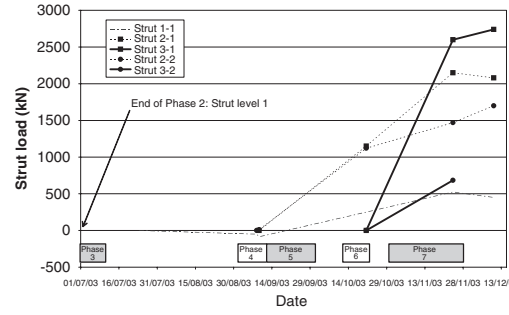

Figure 9. Axial force in the different monitored struts.

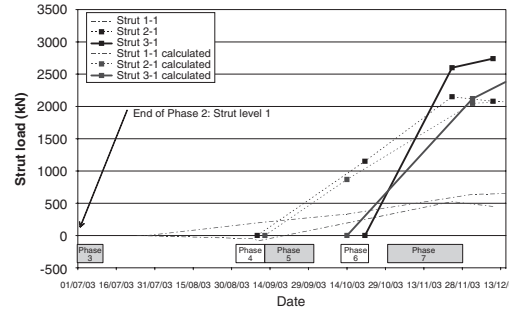

Figure 10. Comparison of calculated and measured axial forces in Struts 1-1 to 3-1.

completion of the excavation works. The chosen dates correspond to (a) stabilized values of the load and (b) to dates of inclinometric surveys.

From the horizontal movement profiles, one can infer the global shortening δ of the different struts. Assuming that δ is only due to variation of axial force in the strut (bending is neglected), the induced load can be calculated from δ and the nominal characteristics of the strut (length 2L, section S and Young's modulus of steel E = 210000 MPa) by:

$$F = \delta \frac{SE}{L} \quad (1)$$

Figure 10 presents the results obtained for Struts 2-1 and 3-1.

Due to the relatively small load that is carried throughout the excavation by Strut 1-1 (approximately 500 kN), a efficiency coefficient smaller than 1 has been introduced in the analysis to represent the non-linearity of the elastic characteristics of the steel. The strut load is thus calculated with:

$$F = \delta \frac{SE}{L} c_{eff} \quad (2)$$

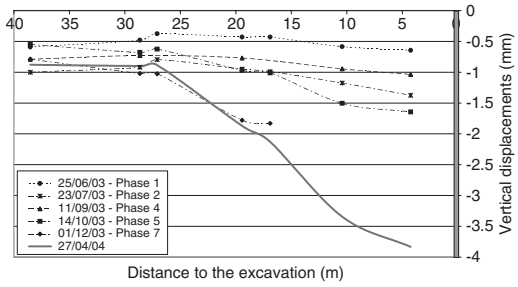

Figure 11. Settlement trough observed on the west side of the instrumented building (points I11 to I17).

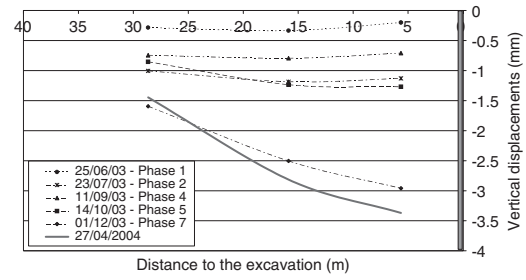

Figure 12. Settlement trough observed on the east side of the instrumented building (points I33 to I37).

In Figure 10, a 50% efficiency coefficient has been chosen. It appears that the calculated values are in good agreement with the measured ones for the three struts and the different excavation phases.

6 SOIL-STRUCTURE INTERACTION

During the excavation, the settlements and horizontal deformations are measured in the one-storey brick building (Section 1).

During the first excavation phases, the settlement troughs observed on the west side of the building (Figure 11) are very different from those obtained in "Greenfield" conditions. It appears that the amplitude of settlements is reduced: a maximum value of 1.65 mm is obtained close to the top of the diaphragm wall at Phase 5. Besides, the shape does not correspond to the spandrel type. Due to technical problems, the settlement trough at the end of Phase 7 (final excavation) is not complete. Nevertheless, after 5 months, the settlements close to the wall are almost equal to those measured in "Greenfield" conditions. The main difference then lies in the extent of the trough: for Section 1, significant settlements are only measured below the brick building with a quasi linear evolution.

From Figure 12, the settlement troughs observed for the eastern façade of the building seem to correspond to a smooth transition between the results of Sections 1 and 2.

The maximum vertical displacement is not influenced by the presence of the light brick building, the building (and its horizontal stiffness) only affecting the width of the settlement trough. Moreover, the global stiffness of the diaphragm wall seems to be equivalent in the two cases even though:

– for Section 1, the large concrete beam reduces the possible deflection of the wall
– for Section 2, the irregular shape of the diaphragm wall increases its stiffness.

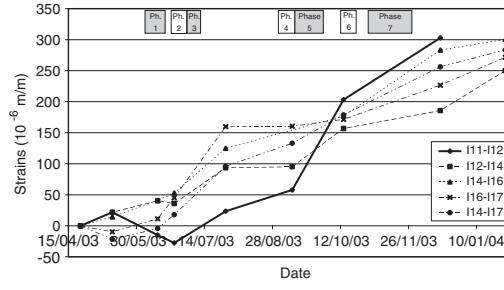

Figure 13. Horizontal extension of the instrumented building.

Horizontal extensions are measured between several anchors installed on the west façade of the building (points I12, I14, I16 and I17, see Figure 3). The results obtained for interval I14–16 and I16–I17 are also checked by the measure of the total extension of interval I14–17. Finally, points I11 and I12 are located on two separate buildings and therefore the measure gives the relative displacement of the two structures.

Figure 13 shows that at the end of the excavation (2 months after completion of Phase 7), the extensions measured for the different intervals are very close (approximately 0.03%), indicating that a global linear horizontal displacement profile is observed in addition to the linear settlement profile of the structure (cf. Figure 11).

Nevertheless, during the 4 excavation phases, the extensions are not uniformly distributed along the structure. Actually, it is only at the end of Phase 4 that the distance between points I11 and I12 increases, indicating a horizontal movement of I12 towards the excavation while I11 remains still.

The total increase of distance between points I11 and I17 is approximately 8.6 mm at the end of Phase 7. At the same time, Figure 5 shows that the deflection of the top of the wall is close to 3.3 mm. The difference can be party explained by measurements errors of

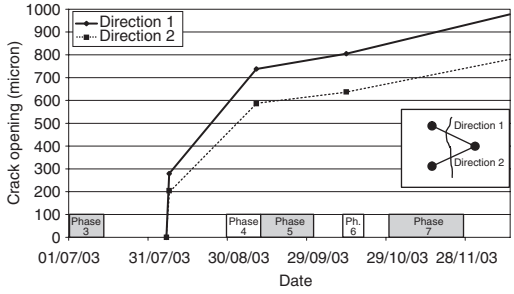

Figure 14. Crack opening measurements (DSAG7).

both the inclinometer and horizontal extension measuring devices. It could also be assumed that there is an approximately 5 mm overall horizontal displacement of the wall itself. Unfortunately, measurements of the horizontal displacements of the wall by total station are not available to check this assumption. Should it be verified, the conclusions drawn from strut loads and wall deflection (see paragraph 5 and Figure 10) would be partly erroneous: an efficiency coefficient would then have to be considered for Struts 2-1 and 3-1 to account for the simultaneous compression and bending behavior of the struts.

Demec strain gauges are also used to determine existing crack opening in the brick building. The 4 cracks that have been equipped (denoted DSAG4 to DSAG7) have an initial width ranging from 0.5 to 1 mm. Figure 14 presents the results obtained for DSAG7 located at the bottom of the western façade of the monitored brick building (Figure 3). The observed movements correspond to a global increase of the crack width of approximately 0.9 mm at the end of the excavation phases. The increase of the distance in Direction 1 is slightly greater than that in the Direction 2. This indicates that in addition to the extension of the crack in the normal direction, it also exhibits a hogging tendency. Opposite results are obtained for DSAG4 located on the other side of the building (with an average crack opening of 0.2 mm) indicating a tendency to sagging. On the whole, there seems to be a twisting movement induced by the differential settlement troughs on either side of the building. DSAG5 and DSAG6 remain unaffected by the structure settlements and horizontal displacements.

7 CONCLUSION

A full set of experimental results have been obtained during the excavation of the 17.2 m deep Saint-Agne subway station. The observed displacements and settlements remain rather limited (compared to the values given in the literature). Possible explanations of these results include the improvement of the construction techniques, the number of struts (and their characteristics) used in this particular case study but also the good mechanical properties of the Toulouse molasses.

It appears that, even though the data include very different physical or mechanical parameters (wall deflection, strut load, settlement, horizontal extension and crack opening), there is a global consistency of these results.

They will be used in further research based on numerical simulations to calibrate the model and analyze the effect of such parameters as the initial K_0 value that seems to be responsible for larger than expected horizontal movements, the stiffness of the existing structure that induces a decrease in the settlement trough width.

In-depth analysis of the variation of the strut loads (axial force and bending moments) will also be carried out as well as a determination of the effect of temperature.

ACKNOWLEDGEMENT

The research project METROTOUL would not have been possible without the kind permission and constant support of the Société du Métro de l'Agglomération Toulousaine (SMAT) represented by Mrs. B. Reynaud.

The authors would also like to thank for the financial support of METROTOUL research program the French Ministry of Research and the Réseau Génie Civil & Urbain (RGC&U). They finally would like to acknowledge the help of the different contractors in collecting data.

REFERENCES

Boscardin M.D. & Cording E.J. 1989. Building response to excavation induced settlement. Journal of Geotechnical Engng., ASCE, Vol. 115, No 1, pp. 1–21.

Burland J.B. 1995. Assessment of risk of damage to buildings due to tunnelling and excavation. Proc. 1st Int. Conf. Earthquake Geot. Eng., IS-Tokyo '95.

Clough G.W. & O'Rourke T.D. 1990. Construction induced movements of in situ walls. Proc. ASCE Conf. on Design and performance of earth Retaining structures, Geotech. Spec. Publ. n° 25, ASCE, New York, pp. 439–470.

Emeriault F., Bonnet-Eymard T., Kastner R., Vanoudheusden E., Petit G., Robert J., de Lamballerie J.-Y. & Reynaud B. 2005. Ground movements induced by earth-pressure balanced, slurry shield and compressed-air tunneling techniques on the Toulouse subway line B. Proceedings of ITA-AITES 2005, 7–12 May 2005, Istanbul, Turkey.

Hsieh P.G. & Ou C.Y. 1998. Shape of ground surface settlement profiles caused by excavation. Can. Geotech. J., Vol. 35, n° 6, pp. 1004–1017.

Long M. 2001. Database for retaining wall and ground movements due to deep excavations. J. Geotech. Geoenv. Eng., Vol. 127, n° 3, pp. 203–2224.

Moormann C. & Moormann H.R. 2002. A study of wall and ground movements due to deep excavations in soft soil based on worldwide experiences. Proc. Geotech. Aspects of Underground Construction in Soft Ground. Kastner et al. (eds), 23–25 October 2002, Toulouse, France, pp. 465–470.

Ou C.Y., Hsieh P.G. & Chiou D.C. 1993. Characteristics of ground surface settlement during excavation. Can. Geotech. J., Vol 30, n° 5, pp. 758–767.

Peck R.B. 1969. Deep excavation and tunneling in soft ground. Proc. Of the 7th ICSMFE, State of the Art Volume, Mexico City, pp. 225–290.

Vanoudheusden E., Petit G., Robert J., Emeriault F., Kastner R., de Lamballerie J.-Y. & Reynaud B. 2005. Impact on the environment of a shallow gallery excavated in Toulouse's molasses by a conventional method. Proceedings of ITAAITES 2005, 7–12 May 2005, Istanbul, Turkey.